Revista Mexicana de Astronomía y Astrofísica, **51**, 11–23 (2015)

INTRAGROUP DARK MATTER DISTRIBUTION IN SMALL GROUPS OF HALOS IN A ΛCDM COSMOLOGY

H. Aceves, F. J. Tamayo, L. Altamirano-Dévora, F. G. Ramón-Fox, R. Cañas & M. Reyes-Ruiz

Instituto de Astronomía, Universidad Nacional Autónoma de México, Ensenada, B. C., Mexico

Received March 14 2014; accepted September 24 2014

RESUMEN

Se estudia la distribución de materia oscura intragrupal en pequeños grupos de halos oscuros de tamaño galáctico en una cosmología ΛCDM. Estos grupos oscuros son identificados utilizando un criterio físico, y pueden ser representativos de pequeños grupos de galaxias. Cuantificamos la cantidad de materia oscura intragrupal y caracterizamos su distribución. Encontramos que las asociaciones compactas de halos, y las intermedias y mucho menos compactas, tienen perfiles de masa oscura algo planos, con pendientes logarítmicas de $\gamma \approx 0$ y ≈ -0.2, respectivamente. Concluimos entonces que la materia oscura intragrupo en estos sistemas no sigue la misma distribución que la de los halos galácticos. En grupos intermedios u holgados de halos la materia intragrupal es $\lesssim 50\%$, mientras que en los compactos es $\lesssim 20\%$ dentro del radio del grupo.

ABSTRACT

We study the distribution of intragroup dark matter in small groups of dark matter galaxy size halos in a ΛCDM cosmology. These groups are identified using a physical criterion and may be an appropriate representation of small galaxy groups. We quantify the amount of intra-group dark matter and characterize its distribution. We find that compact associations of halos, as well as intermediate and loose groups, have rather flat intragroup dark matter profiles, with logarithmic slopes of $\gamma \approx 0$ and ≈ -0.2, respectively. Hence, the intra-group dark matter of these halo systems does not follow the same cuspy tendency of galactic halos. In intermediate and loose associations of galaxy-size halos, the intragroup matter tends to be $\lesssim 50\%$ of the total mass of the group, while in compact associations it is $\lesssim 20\%$ of the mass within their group radius.

Key Words: dark matter — galaxies: clusters: general — galaxies: halos — large-scale structure of universe — methods: numerical

1. INTRODUCTION

The formation of structures is a general characteristic of the gravitational interaction between particles in the universe, regardless of the cosmological model one uses to describe it. The details of how the growth of structures proceeds in a simulation depend, however, on the adopted cosmological model. It is an observational fact that a large percentage of galaxies at lower redshifts are found in aggregates ranging from small groups to large clusters of galaxies (e.g. Holmberg 1950, Tully 1987, Nolthenius & White 1987, Eke et al. 2004).

The importance of understanding groups of galaxies and the evolution of galaxies within such environments was the main motivation for early catalogs such as those of (Tully 1980) and (Huchra & Geller 1982), and of more recent observational efforts, including those that aimed to determine the distribution of mass in groups and clusters of galaxies (e.g. Eke et al. 2004, Brough et al. 2006, Berlind et al. 2006, Yang et al. 2007, Tago et al. 2010, Calvi et al. 2011, Carollo et al. 2012, Williams et al. 2012, Domínguez-Romero et al. 2012, Tempel et al. 2014).

In studies of small groups of galaxies, in particular compact ones (e.g. Hickson 1997, Tovmassian et al. 1999, Allam & Tucker 2000, de Carvalho et al. 2005, Niemi et al. 2007, McConnachie et al. 2008, Mamon 2008, Díaz-Giménez et al. 2012),

a recurrent topic is the abundance of physical groups and the explaination of their "existence" given their small crossing times. Dynamical studies (e.g. Barnes 1989, Athanassoula, Makino & Bosma 1997, Gómez-Flechoso & Domínguez-Tenreiro 2001, Aceves & Velázquez 2002) have shown that compact groups may have a long existence, given their initial conditions. Cosmological simulations (e.g. Diaferio et al. 1994, Governato et al. 1996, Casagrande & Diaferio 2006, Sommer-Larsen 2006) have also addressed the question of compact groups, including some of the baryonic gas physics. The comparisons of observed compact associations (CAs) with galaxy mock catalogs led to the conclusion that a significant fraction (about 30%) of tha observed compact associations found in observational catalogs are physical systems (e.g. McConnachie et al. 2008, Mamon 2008, Díaz-Giménez & Mamon 2010), with different percentages depending on the details of the selection criteria used for constructing the mock catalogs (e.g. Duarte & Mamon 2014). The problem of the longevity of small compact groups is still an open question.

The amount and distribution of luminous and dark matter in the various structures found in the universe, from galaxies to clusters, is an important problem and may serve to discriminate or impose restrictions to cosmological models. The intracluster light observed in, for example, the Coma Cluster and other clusters (e.g. Zwicky 1951, Gonzalez et al. 2000) suggests that it might be 10 to 50 percent of the total light of such structures. Intragroup diffuse light has also been observed in some Hickson's compact groups for which different percentages have been suggested; e.g., for HCG44 about 5 percent of the total light (Aguerri et al. 2006), and for HCG95 and HCG79 about 11 and 45 percent respectively (Da Rocha & Mendes de Oliveira 2005).

The content and distribution of dark matter is more or less well established in large structures, such as clusters, by observations and analysis of gravitational lensing (e.g. Bartelmann 2010, Newman et al. 2012), among other methods. (Sand et al. 2004) found that the distribution of dark matter in some clusters of galaxies is inconsistent with the NFW profile. There are almost no studies in the mass range of small groups, $M_g \approx 10^{13} M_\odot$, due primarily to observational limitations. The amount and distribution of dark matter in small groups is important, for instance, for dynamical studies of the interactions between galaxies in such environments. Several authors have investigated the mass content of galaxy groups using lensing methods (e.g. Hoekstra et al. 2001, Parker et al. 2005, Limousin et al. 2009, Thanjavur et al. 2010, McKean et al. 2010), thus avoiding the complications of other methods that depend on the dynamical state of the system or on its gas temperature. In particular, (Thanjavur et al. 2010) found that dark matter is distributed in a cuspy manner in groups whit a mass close to $10^{14} M_\odot$, while (Hoekstra et al. 2001) found a tendency towards an isothermal profile for another set of groups (CNOC2 groups, Carlberg et al. 2001) with a lower mass of $\approx 10^{13} M_\odot$.

The purpose of this work is to quantify and characterize the amount of diffuse or intra-group (IG) dark matter in small groups of galaxy-size dark matter halos; i.e., the dark matter not bound to well-defined virialized halos, which is estimated to be in the mass range of $M \in [10^{11}, 5 \times 10^{12}] h^{-1} M_\odot$. This with the aim of obtaining an estimation of what could be expected in true physical small galaxy groups, since these halos can host normal galaxies. We studied this type of distribution of dark matter using a set of five cosmological simulations within the ΛCDM cosmology (§ 2.1). Bound groups of halos were identified using a physically motivated algorithm that allowed for an unambiguous identification of groups in our simulations (§ 2.2). The membership to a small dark group was determined by considering only halos that could host "normal" galaxies (§ 2.2.2). In the analysis of the simulations, we differentiated, as it is done in observational studies, between compact associations, and intermediate and loose groups, by means of the size of the group radius $R_{\rm g}$.

The outline of the paper is as follows. In § 2 we describe our simulations and the methods used in this study, such as the algorithm used to determine which halos belong to a dark group or not. In § 3 we present our results regarding the amount and distribution of intragroup (IG) dark matter, as well as the evolution in time of the IG dark matter profile for compact associations of galaxies. In § 4 we make some final comments on our work.

2. METHODOLOGY

2.1. *Cosmological Simulations*

Our groups of halos were obtained from a set of five similar cosmological simulations within the ΛCDM model, each differing from each other in the random seed used to generate the initial conditions. The cosmological parameters used are consistent with those of the WMAP7 results (Larson et al. 2011, Table 3), from where we took matter density $\Omega_m = 0.27$, dark energy density $\Omega_\Lambda = 0.73$, spec-

tral index $n_s = 0.963$, mass fluctuation $\sigma_8 = 0.816$ and a Hubble parameter $h = 0.70$. Each simulation box had a comoving length of $L = 100\,h^{-1}$ Mpc with $N_p = 512^3$ dark matter particles, each particle having a mass of $m_p \approx 6 \times 10^8 h^{-1}\,M_\odot$.

Initial conditions were generated using 2nd-order Lagrangian perturbation theory (e.g. Crocce, Pueblas & Scoccimarro 2006) at a redshift of $z = 50$. This value is sufficiently large to avoid the effects of transient modes that result from a truncation in perturbation theory at redshifts of $z \approx 5$ (e.g. Tatekawa & Mizuno 2007). However, for halos in the range of $M \in 10^{10-13} h^{-1}\,M_\odot$, it appears that first and second order perturbation methods at $z = 0$ do not make an important difference in halo properties (Knebe et al. 2009). The initial linear power spectrum density was calculated using the transfer function from the cosmic microwave background code CAMB (Lewis, Challinor & Lasenby 2000), normalized so that it gave the current mass fluctuation σ_8 value shown above.

The N-body cosmological simulations were carried out using the publicly available parallel Tree-PM code GADGET2 (Springel 2005). The simulations were run with code parameters similar to those identified as "high quality" (HQ) in the simulations of (Crocce et al. 2006); for example, using a softening length of $\varepsilon = 20 h^{-1}$ kpc. Since we were not interested in small halo substructures, but rather on the dark halos of typical normal galaxies with virial radii of ≈ 200 kpc, we did not expect important differences in our group finding methods of such parameters as a function of the softening funtion. We were able to test and verify this by re-doing three similar simulations but with $\varepsilon = 20 h^{-1}$ kpc.

2.2. *Halos and Group Identification*

2.2.1. *Halos*

There are several halo finders, and many of them have been recently compared (Knebe et al. 2011), but newer ones were excluded from that comparison study (e.g. Elahi, Thacker & Widrow 2011, Han et al. 2011). We chose the Amiga Halo Finder (AHF, Gill et al. 2004 and Knollmann & Knebe 2009) as our dark matter halo (DMH) identification algorithm, which uses an adaptive mesh to look for bound particle systems. In order to have well defined halos not much subject to numerical noise, we selected halos with a minimum number of particles of $N_p = 100$, which in our simulations correspods to halos with masses of $M_{\rm min} \approx 6 \times 10^{10} h^{-1}\,M_\odot$. The output of the AHF code provides, among other things, the viral mass and radius of halos and subhalos.

2.2.2. *Groups*

As noted in § 1, it was not our purpose here to make a mock catalog of small galaxy groups, loose or compact, or to make a direct comparison with observations. Our objective was to determine *physically* bound small groups of halos in our ΛCDM cosmological simulations; these groups, nonetheless, may resemble small galaxy groups with respect to the distribution of their intragroup dark matter. In order to carry out our objetive, we defined clear physical quantities in our search algorithm. We proceeded as follows to determine a group of halos that could probably host "normal" galaxies.

First, considering the galaxies of our Local Group as typical of a small galaxy group environment, we determined a halo mass that could be associated with a galaxy like M33. This galaxy was considered as our fiducial lowest total mass for a "normal" galaxy. Using the monotonic mass-luminosity relation of (Vale & Ostriker 2004), with an absolute magnitude of $M_V = -18.9$ for M33 (Mo, van den Bosch & White 2010), we estimated a total mass of $M_{\rm min} \approx 10^{11} h^{-1}\,M_\odot$, which is consistent with the value used by (Berlind et al. 2006) with a Halo Occupation Distribution fitted to the SDSS two-point correlation function of galaxies of such luminosity. Thus, we took $M_{\rm min}$ as the lowest mass of the dark halo of a normal galaxy that could be considered as part of a group of halos. The upper mass was set to be about twice that of the Milky Way, with $M_{\rm max} \approx 5 \times 10^{12} h^{-1}\,M_\odot$. Thus, in our simulations we used halos in the mass range $M \in [M_{\rm min}, M_{\rm max}]$ as a criterion to determine membership in a small group of halos. In other words, our approach prevented smaller subhalos from defining a group of galaxy-size halos and very massive single halos ($M \gtrsim M_{\rm max}$), which are not found in small galaxy groups; we dis not consider fossil groups that may host a cD-type galaxy.

Secondly, we used a simple search algorithm to determine our physical groups of halos at $z = 0$. This algorithm required that the number of galaxy-size halos $N_{\rm h}$ to be $N_{\rm h} \in [4, 10]$ and within a physical radius of $R_{\rm max} = 1\,h^{-1}$Mpc from the center of mass of the tentative members, and that no other normal galaxy-size halo be within $R_{\rm n} = 1.25\,R_{\rm max}$. The chosen radius $R_{\rm max}$ more or less corresponded to the turn-around radius (Gunn & Gott 1972) with a mass of $\approx 10^{13} M_\odot$, and $R_{\rm n}$ was set only to provide a clear physical isolation criterion from other possible bound structures nearby; see Figure 1. We applied this group-search algorithm successively to all dark halos that had $M \in [M_{\rm min}, M_{\rm max}]$ in the simulations.

This procedure generated a set of group candidates with radius $R_{\rm g}$; measured from the center-of-mass of the galaxy-size halos to the center of the outermost one.

In order to differentiate several degrees of compactness found in the dark groups, we refer to the groups with a spherical radius $R_{\rm g} < 250\,h^{-1}\,$kpc as compact associations (CAs, or compact groups for simplicity), intermediate associations (IAs) to those systems with $R_{\rm g} \in (250, 500)\,h^{-1}\,$kpc, and loose associations (LAs, or loose groups) for groups with $R_{\rm g} \in [500, 1000]\,h^{-1}\,$kpc.

The insolation degree of our previous set of group candidates needed to be further adjusted in the cosmological simulations in order to have a cleaner sample of isolated groups. This was specially needed for LAs since some of them had larger structures within $\approx 1\,h^{-1}$Mpc of its outermost halo. All of the CAs satisfied an isolation criterion (similar to that of Hickson) of not having a galaxy-size dark halo within $3R_{\rm g}$, since the maximum group radius of CAs satisfies, by definition, $3R_{\rm g} < R_{\rm max}$, so no further modifications to the algorithm were required. For both IAs and LAs we imposed a further restriction that no other dark halo would be within $R_{\rm g} + R_{\rm max}$ from their center. This allowed us to have a well isolated sample of IAs and LAs.

Finally, we checked that all groups identified using the above procedure were actually bound systems by approximetely estimating their kinetic and potential energy as if the halos were point particles, and the intragroup matter was negligible. The kinetic energy of the group was computed as follows:

$$T = \frac{1}{2M}\sum_{i<j} M_i M_j (\mathbf{V}_i - \mathbf{V}_j)^2\,, \qquad (1)$$

with M being the total mass of the group of virialized halos, M_i that of the i-th halo, and $\mathbf{V}_i$ the corresponding velocity. The potential energy was calculated as

$$U = -G\sum_{i<j} \frac{M_i M_j}{R_{ij}}\,, \qquad (2)$$

where R_{ij} is the physical separation between two halos. We considered the group to be bound if $T < |U|$. A similar approach was used by (Niemi et al. 2007) to discriminate bound from unbound groups of halos. All groups of halos identified in the previous step were bound. The average virial ratio of all of our groups was $\langle 2T/|U|\rangle = 0.14 \pm 0.33$, while for CAs it was 0.03 ± 0.08. As shown in § 3, all CAs found in the cosmological simulations were in state of collapse, consistent with their low average virial ratio.

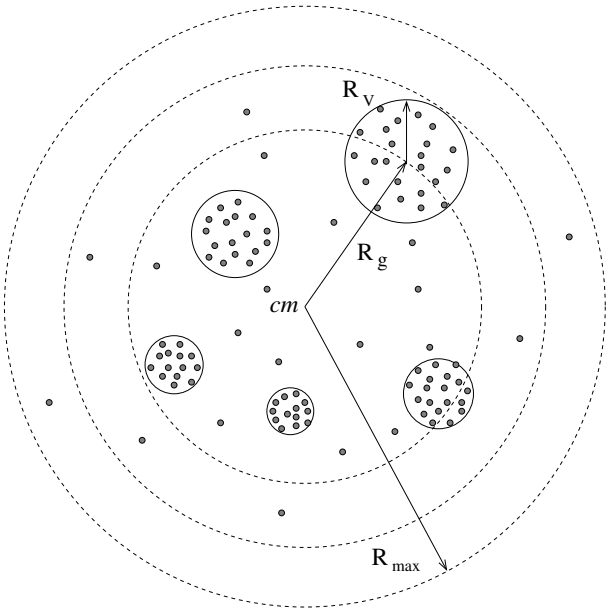

Fig. 1. Schematic diagram of different quantities used to determine our physical groups. Matter not bound to individual halos with virial radius $R_{\rm V}$, was considered to belong to the intragroup medium if it was also located within $R_{\rm max} = 1\,h^{-1}$Mpc from the center-of-mass (cm) of the group. The group radius, $R_{\rm g}$, is determined by the radius of an imaginary three-dimensional sphere centered on its center-of-mass and extending up to the center of the furthest galaxy-size halo.

A way to assign luminosity to the dark halos would be required in order to compare with observational catalogues (e.g. Casagrande & Diaferio 2006, McConnachie et al. 2008, Díaz-Giménez & Mamon 2007, and Niemi et al. 2007). However, that is out of the scope of the present work.

It is known that different identification criteria lead to different numbers of galaxy associations indentified in a simulation or in the sky (e.g. Duarte & Mamon 2014). In our method we selected groups of halos by mimicking, in a simple way, the procedure used to determine galaxy groups (e.g. Lee et al. 2004). Namely, we looked for associations of dark halos within a certain spatial region without making any assumptions beside considering galaxy-like mass halos. Then we verified that they were truly physically bounded groups and explored their properties. Other recent approaches (e.g. Berlind et al. 2006, Yang et al. 2007, Domínguez-Romero et al. 2012) essentially go the other way around, looking for dark halos in a particular mass range ($\approx 10^{13} h^{-1}\,M_\odot$)

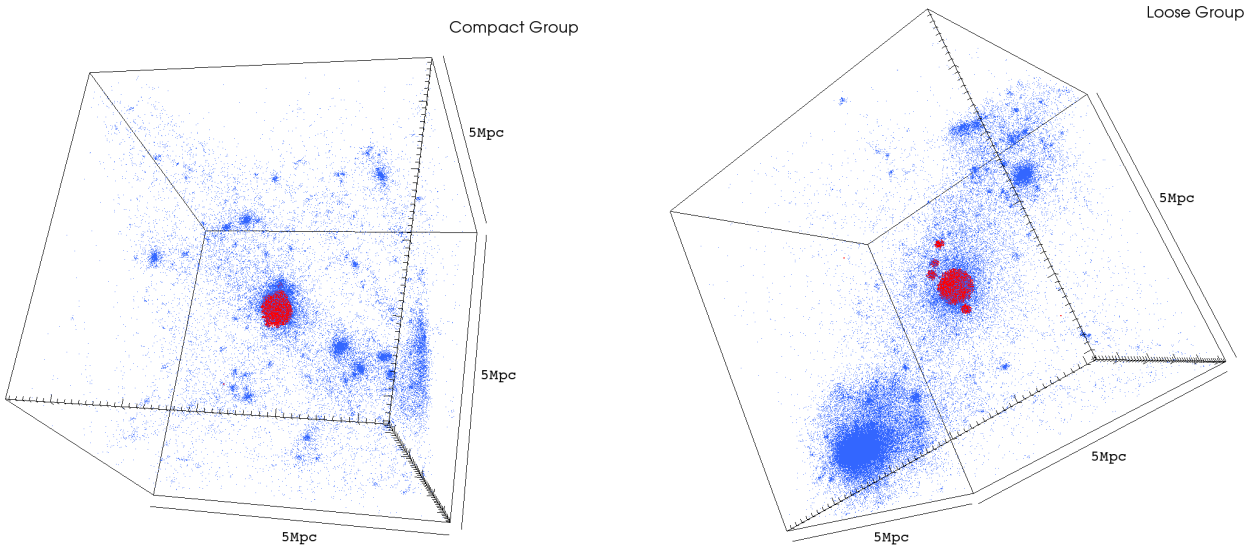

Fig. 2. An example of a compact (*left*) and loose (*right*) group association of halos. The red dots indicate particles belonging to halos that satisfy our group criteria, while blue dots refer to particles belonging to the intragroup medium; other structures not belonging to these groups are also shown. The two small dark halo groups are physically bound objects, not projected systems. The color figure can be viewed online.

and studying their properties and content (subhalos). We will discuss here briefly these differences with our approach and study how they relate to our results.

Finally, to quantify the distribution of intragroup dark matter, we removed all particles not associated with individual halos, as signaled by the AHF code, then measured its amount and determined its distribution with respect to the group center-of-mass. The total intragroup mass was determined both within the group radius $R_{\rm g}$ and within the estimated turn-around radius $R_{\rm max}$. We traced the evolution of particles in CAs from $z = 0.5$ to $z = 0$; all remained within the $R_{\rm max}$ radius. We estimated the mass density profile, in particular its inner slope, assuming spherical symmetry for the IG dark matter, and stacking approximately the same number of IG particles for CAs and LAs.

3. RESULTS

Figure 2 shows the location of two small dark groups found in one of our cosmological simulations. In red we show the particles associated with halos of galaxies belonging to a group according to our selection criteria, and in blue we show the matter not associated with the DMHs of the group. Figure 2 shows only compact (*left*) and loose (*right*) associations of halos. A visual inspection of the simulations showed that most of our groups are found in filaments of the large-scale structure (e.g. Hernquist et al. 1995), although some of them are near larger cluster-like structures at the nodes of the cosmic web. None was found in what might be called voids. All results are consistent with the general trend of observations of small galaxy groups (e.g. Godłowski & Flin 2010, Mendel et al. 2011). Table 1 shows the average values and standard deviation of the total mass (halos and IG matter), radius of the group, three-dimensional velocity dispersion and dimensionless crossing time of our associations.

A total number of 14 objects classified as CAs, a set of 64 IAs, and a total of 661 LAs were found in our five cosmological simulations at $z = 0$. In particular, the average number of CAs per simulation was $\langle N_{CA} \rangle \approx 3$ in our simulation box of volume $(100\,h^{-1}{\rm Mpc})^3$. This number of CAs appears to be rather low when compared with the results of other authors. Scaling these numbers to boxes such as the one used in the *Millennium Simulation* (*MS*, Springel et al. 2005), of side length $L = 500\,h^{-1}$ Mpc, that is, multiplying our numbers by a volume correction factor of 5^3, we found about 1/3 of the CAs found, for example, by (McConnachie et al. 2008) who found ≈ 1200 groups in the *MS*; however if another search algorithm is used, the numbers are significantly different.

We tested if the use of a higher value of $\sigma_8 = 0.91$, such as that used in the *MS* (compared to the value used here $\sigma_8 = 0.82$), might have lad to more group-scale structures and, hence, to better agreement with

TABLE 1

GLOBAL PROPERTIES OF DARK HALO GROUPS

	M $10^{12}h^{-1}\,M_\odot$	$R_{\rm g}$ $h^{-1}\,$kpc	σ km/s	t_c/t_H
CAs	9.23 ± 2.23	211.2 ± 35.7	296.0 ± 59.9	0.038 ± 0.010
IAs	7.46 ± 4.88	419.2 ± 61.9	296.3 ± 142.2	0.088 ± 0.041
LAs	8.01 ± 4.77	827.5 ± 121.9	263.2 ± 150.2	1.349 ± 18.032

other studies that used the *MS* results. We made two additional cosmological simulations using the same cosmological parameters as those used in the *MS* (e.g. $\Omega_m = 0.3$, $\Omega_\Lambda = 0.7$ and $\sigma_8 = 0.91$) but in a box of length $L = 100\,$Mpc/h and with 512^3 particles.

Using the same analysis of our two simulations above to identify CAs, we found an average of $\langle N_{CA}\rangle_{MS} = 10$. This increase of CAs in the *MS*-like simulations was consistent with the expected result when a higher σ_8 was used in a cosmological model, although we were dealing with small-number statistics. After correcting by the volume factor indicated above, the number of CAs was similar to those of other authors for these type of groups using similar selection criteria but including luminosity related properties (e.g. Casagrande & Diaferio 2006, McConnachie et al. 2008, Díaz-Giménez & Mamon 2007, Niemi et al. 2007). There might be other differences of lower order due to, for instance, using a friends-of-friends criteria (e.g. McConnachie et al. 2008) when fixing the size of the linking length l of the "friendship" (e.g. Duarte & Mamon 2014), or to lowering the observational threshold "magnitude" of detection in groups in mock catalogs.

3.1. *Amount of IG dark matter*

As indicated in § 2 we identified dark matter particles associated with an intragroup environment as particles not physically bound to the halos identified using the AHF code; first all particles within a $R_{\rm max} = 1\,h^{-1}$Mpc radius and then within $R_{\rm g}$. Figure 3 shows the frequency of the ratio of IG dark matter to total group mass, f, for our loose associations and for the intermediate ones, using the indentification criteria for both groups. The average total IG mass obtained for all three types of groups found, and that of the matter in halos, was $\langle M\rangle \approx 8\times10^{12}h^{-1}M_\odot$.

The median values of these ratios, within $R_{\rm max}$, were $\hat{f}_{\rm L} = 0.40$ and $\hat{f}_{\rm I} = 0.42$ for our loose and intermediate associations, respectively. For compact associations we found an average value of $\langle f\rangle_{\rm C} = 0.41$, but it is not shown as a histogram in Figure 3 since we only have a few points. In general, the amount of IG dark matter tended to be less than $\approx 50\%$ of that of the whole bound system, with a median of $\approx 40\%$, irrespective of the configuration of the group if the size of the group was taken to be $R_{\rm max}$.

When we counted only matter within the group radius $R_{\rm g}$ for CAs, we obtained $\langle f\rangle_{\rm C} = 0.20$, while for IAs and LAs we found the corresponding fractions to be $\hat{f}_{\rm I} = 0.26$ and $\hat{f}_{\rm L} = 0.38$, respectively. As noted, the difference between the two ways of determining the size of the group as related to the fraction of intragroup dark matter tended to decrease for loose associations and became significantly different for compact groups.

It is worth noting that within the group radius $R_{\rm g}$, specially in compact configurations, a lot of dark matter particles find their way into bound structures, thus reducing the intragroup medium, since the latter is defined by particles not bound to any halo of the member galaxies. This behavior was noted also in the density profiles computed in the next section. Some matter may also be associated to smaller subhalo type structures, but we did not distinguish here between dark subhalo particles and intragroup particles.

3.2. *IG dark matter profiles*

In Figure 4 we show the stacked distribution of about 39,000 IG dark matter particles of compact associations found in our simulations at $z = 0$ according to our selection criteria. A similar plot, but for loose groups, is shown in Figure 5; here $\approx 35,000$ particles are shown. The scale of both figures is the same in terms of the group radius of the associations. The centers of mass of all stacked groups coincide. We should mention that no galaxy-size dark halo was found to reside at the center of mass of a group in our search algorithm.

Both Figures 4 and 5 show no indications of a central concentration of intragroup dark matter and

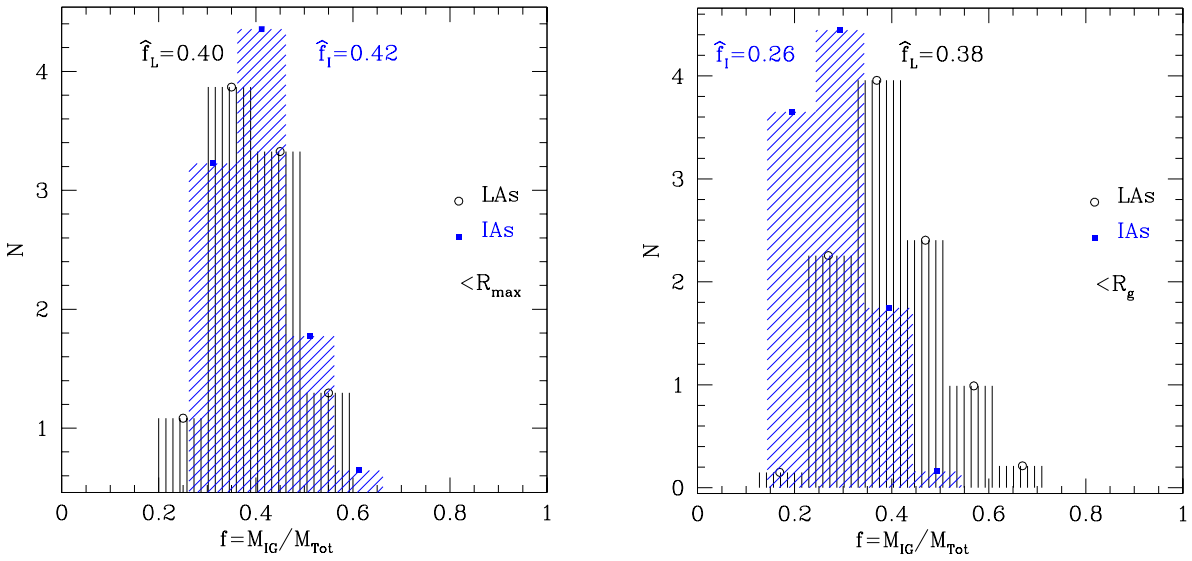

Fig. 3. Frequency distribution of intragroup dark matter according to total mass in our small group-like objects, both within $R_{\rm max}$ (*left*) and the radius $R_{\rm g}$ (*right*). Median values are indicated for loose and intermediate associations. For compact associations, we obtained an average value of $\langle f \rangle_{\rm C} = 0.41$ in the first case and $\langle f \rangle_{\rm C} = 0.20$ in the second one.

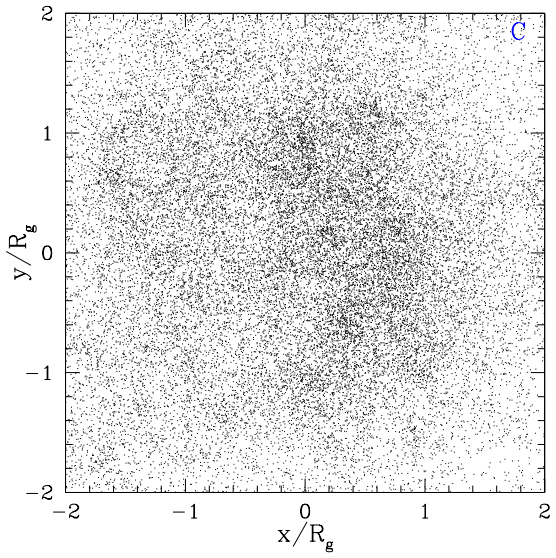

Fig. 4. Stacked distribution of the IG dark matter of small groups of dark matter halos that have a compact configuration. The total number of particles shown are 39,231 and the thickness of the box is $4R_{\rm g}$.

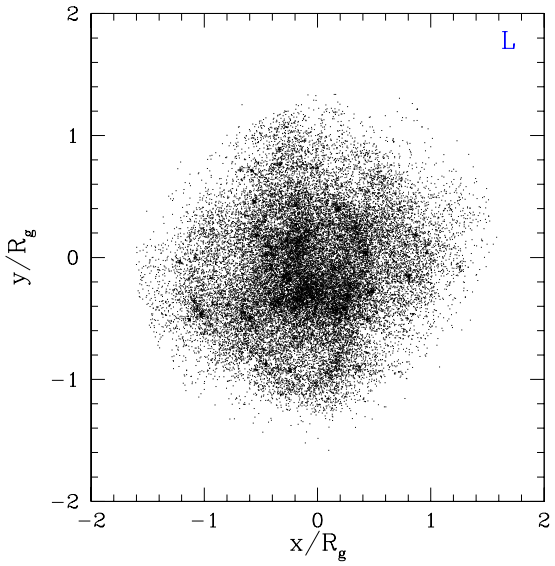

Fig. 5. As in Figure 4 but for loose groups. Plotted are just 34,112 IG dark particles to aid in viewing some residual structures in the dark matter; i.e. not considered to be bound halos due to our selection criteria.

show a behavior more akin to an homogeneous distribution; the same behavior was observed for the intermediate associations. In these plots we have taken all the particles belonging to halos with $N_{\rm p} \geq 100$ out of the accounting, but smaller concentrations appear in them.

To quantify the degree of concentration of the IG dark matter we computed the spherically-averaged density profile $\rho(r)$ of all particles belonging to compact, intermediate and loose associations; the profiles are centered on the center-of-mass of the group as defined earlier. When comparing $\rho(r)$, all coor-

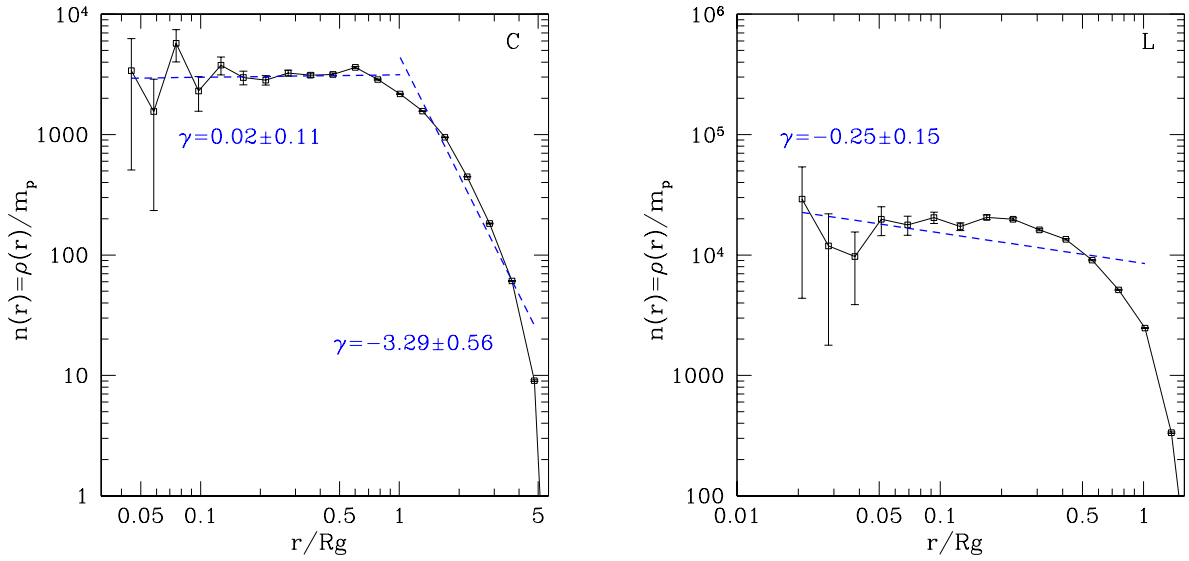

Fig. 6. IG dark matter density profile of compact (CAs, *left*) and loose associations (LAs, *Right*). Compact groups of galaxy-size dark halos show an inner power-slope of $\gamma = 0.02 \pm 0.11$ at $r \leq R_{\rm g}$, with a rapid density decay afterwards. Loose groups up to their $R_{\rm g}$ yield a $\gamma = -0.25 \pm 0.15$ slope.

dinates of particles have been scaled by the group radius to which they belong.

In Figure 6 (*left*) we show the mass density profile of the IG-DM for compact associations. A power-slope fit, $\rho \propto r^{\gamma}$, was made yielding a value of $\gamma = 0.02 \pm 0.11$ for the inner part $r \leq R_{\rm g}$, and an external slope ($r \in (R_{\rm g}, 5R_{\rm g}]$) of $\gamma = -3.29 \pm 0.56$ was obtained. Errors in the slopes of the profiles in the fits were estimated in all cases by a bootstrap method (Efron & Tibshirani 1993). Error bars at the data points are Poisson errors.

In Figure 6 (*right*) we show the IG dark matter profile for those groups identified as loose. An internal power-slope fit yields $\gamma = -0.25 \pm 0.15$; no fit is made after $R_{\rm g}$ since for these groups $R_{\rm g} \approx R_{\rm max}$, where the density falls rather sharply after $R_{\rm g}$.

The profiles shown in Figure 6 have a minimum starting radius at about the scale of the softening radius ($\varepsilon = 20h^{-1}$kpc), in terms of the average group radius for the halo associations shown. In order to explore the effect of the softening radius on the inner slope of the halo associations, we made two additional cosmological simulations but with $\varepsilon = 1h^{-1}$kpc. For six CAs identified in these new simulations, after stacking them, we obtained an inner slope of $\gamma = 2.09 \pm 0.18$ and an external one of $\gamma = -4.01 \pm 0.37$, and for the 273 LAs an inner slope of $\gamma = 0.30 \pm 0.13$ results. The deficiency of IG dark matter in this sample of CAs, with inner slope $\gamma \approx 2$, is also noticed in several systems of the first set of simulations. The two old simulations similar to the new ones both use the same initial seed to construct the initial conditions and yield an inner slope of $\gamma = 1.84 \pm 0.13$ for these six groups. The two inner slopes for the CAs, for the two different softenings considered here, are consistent with each other; the same is observed for the outer slopes. However, the value reported above using $\varepsilon = 20h^{-1}$kpc results from stacking more associations and can thus be considered to represent an average behavior in a typical system of this kind. Nonetheless, the previous situation is indicative of the complexity of the inner distribution of dark matter in compact associations of galaxy-size dark halos.

It follows, however, from the above results that the IG dark matter does *not* tend to be cuspy in any kind of halo associations found here, and also that it does not dominate the mass.

3.3. *Evolutionary trends*

In Figure 7 we show the time evolution of the configuration, at different redshifts, of a particular compact group of halos of one of our simulations. As observed, the CA at $z = 0$ results from the collapse of a loose group, and no other normal galaxy enters a sphere of $R_{\rm max}$. The dynamical state of the whole group is that of a collapse, that has not had time to completely merge. The same trend is observed for other CAs in our simulations, as shown graphically in Figure 8, where we plot the group radius from $z = 1$ to $z = 0$ for our CAs.

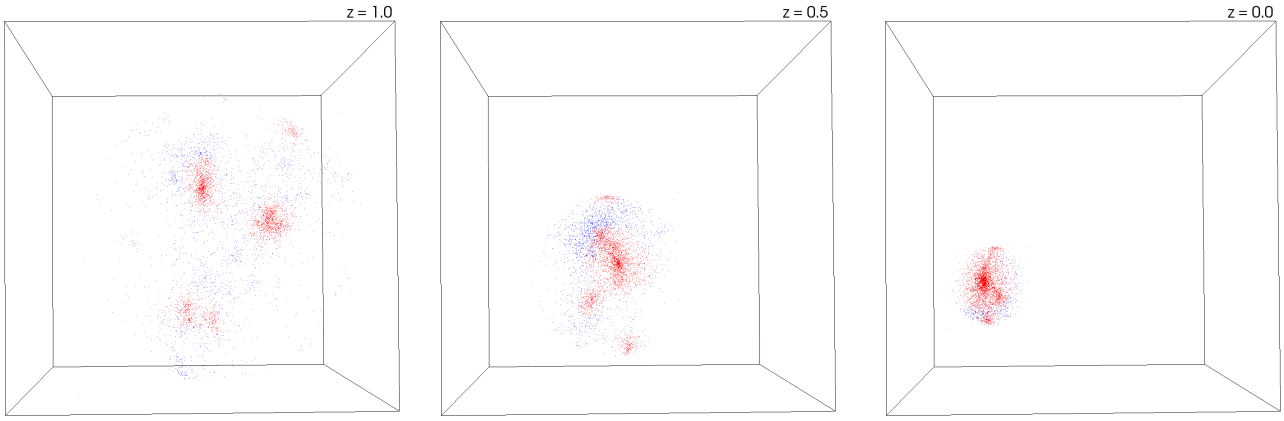

Fig. 7. Evolutionary sequence of a particular compact group, at $z = 1.0$, $z = 0.5$ and $z = 0$. The box has $2\,h^{-1}$ Mpc on each side. Red points correspond to particles associated with galaxy halos while blue ones to intragroup dark matter. The color figure can be viewed online.

We also computed the crossing times of our groups of halos. The average dimensionless crossing time is $t_c/t_H \approx 0.03$ for CAs and ≈ 0.2 for LAs; where $t_c = R_g/\sigma$ is a physical crossing time, t_H is the Hubble time, and σ is the three-dimensional velocity dispersion of the group. An observational equivalent to t_c, after projecting along a line-of-sight, is typically used in observational studies (e.g. Hickson 1997). (Berlind et al. 2006) find a median value of the dimensionless crossing time $t_{cross} \approx 0.15$ for their group catalogs which include systems of a wide range of sizes and velocity dispersions; their crossing time is related to our deprojected value by $t_c = 4/(\pi\sqrt{3})t_{cross}$. On the other hand, for compact groups typically one has $t_c/t_H \sim 0.01$. Hence, our values for t_c are within the range found by other authors.

One might think, based on our dimensionless crossing times, that the halo groups are in virial equilibrium, but this is not the case. (Aceves & Velázquez 2002) showed that the value of the crossing time is not necessarily a good estimator of the dynamical state of a group. These authors found, using dynamical studies of groups, that one can have small values of the dimensionless crossing times for collapsing groups that were clearly not in virial equilibrium; as indicated in their Figure 4. In our cosmological simulations the average virial ratio for all associations is $\langle 2T/|U|\rangle = 0.46 \pm 0.22$ and for compact associations it is 0.03 ± 0.04. From the crossing time results and the virial estimator used, it follows that the former does not appear to be a solid parameter to determine if a group of the kind considered here is in virial equilibrium. The same argument may probably apply to observational galaxy groups, but this matter deserves further work.

In order to see if evolutionary trends in the slopes of the IG dark matter exist, we computed the density profile for all of our CAs at three different redshifts: $z = 1.0$, $z = 0.5$ and $z = 0$. The results of the mass profile are shown in Figure 9. The average inner slope of the IG dark matter is essentially flat, within the estimated errors, from redshift $z = 1$ to $z = 0$. The IG dark matter appears to be more confined within R_g at the higher redshifts than at $z = 0$, as a consequence of the general collapse of the group of halos. The galaxy-size halos project the IG particles toward the external parts of the group by transferring kinetic energy to them. This was observed by visually following the IG dark particles from $z = 1$ to $z = 0$ for all of our CAs. One may notice a hint of the latter by observing the IG dark particles in Figure 7.

4. FINAL COMMENTS

By using a set of ΛCDM cosmological simulations, with parameters in agreement with recent results from the WMAP7 observations, we studied the distribution of dark matter in the intragroup environment of small associations of galaxy-like halos.

In general we found for intermediate or loose groups that physically well-defined halo structures, that may resemble small groups of galaxies, have on average $\lesssim 40$ percent of the total mass of the system in an intragroup medium, and that the rest resides in bound halos. For compact associations the fraction of intra-group dark matter within the group radius (R_g) is about 20% of the total group mass. Interest-

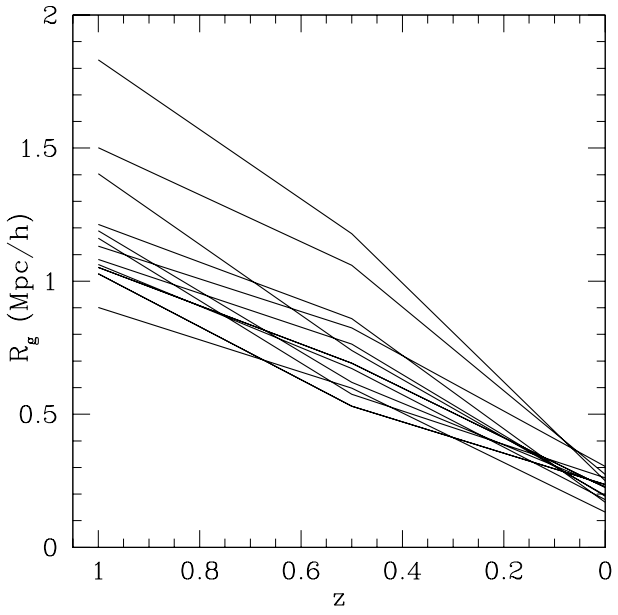

Fig. 8. Comoving group radius as a function of redshift for our CAs. The sizes were determined at $z = 1.0, 0.5$ and $z = 0$. All CAs at $z = 0$ result from a collapsing state at a higher redshift.

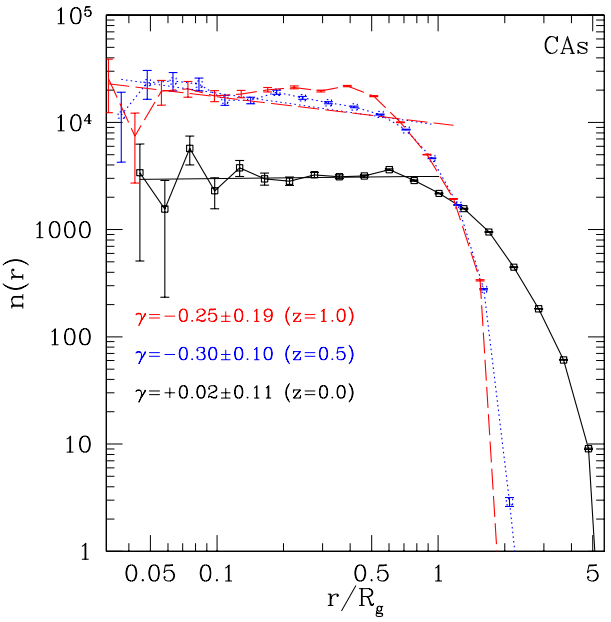

Fig. 9. Evolution in time of the intragroup dark matter profile for compact associations up to $5R_g$ from $z = 1$ to $z = 0$. The inner ($r < R_g$) logarithmic slope tends to remain constant within the uncertainties. The distribution of IG dark particles is more extended at $z = 0$.

ingly enough, these amounts of dark matter are comparable to the amounts ($\approx 10 - 50\%$) of intracluster light found in observational studies of related astronomical systems. However, their nature appears to be different. Intracluster light comes from tidally stripped stars from galaxies, while our intragroup dark matter is the dark matter of the halos that surround galaxies. It will be of interest in the future to measure the amount of intragroup light in simulations that include a baryonic component, and to compare it with observations.

Aside from the rather small amount of IG dark matter for groups, we found that their distribution is rather flat. An *average* logarithmic slope of $\gamma = 0.02 \pm 0.11$ in the central parts ($r \leq R_g$) of CAs was found, while for LAs $\gamma = -0.25 \pm 0.15$ was obtained. In no case was a single halo dominant or resided at the center-of-mass of our groups of dark matter halos. In some CAs we found a deficit of dark matter particles in the central parts, even after diminishing the softening radius of a cosmological simulation to $\varepsilon = 1h^{-1}$ kpc. A better estimate of the dark matter profile at such scales would certainly need to increase the number of particles in the cosmological simulations or do a re-zooming in the region of interest. However, the latter possibilities were not explored in this work. On the other hand, the intragroup dark matter distribution in a particular group of halos appears to depend on its aggregation history in a complex manner.

All of our results indicate that the distribution of dark matter in such halo associations does *not* follow a cuspy (e.g. a NFW) profile, contrary to what happens in individual halos formed in a ΛCDM cosmology. This result is consistent with the gravitational lensing results of (Hoekstra et al. 2001) that use groups of masses similar to the ones considered here. Hence, the structure of what can be called a common halo of a small galaxy group might bear little resemblance to the halos of its constituent galaxies.

The results of this work may be also relevant to works related to the dynamics of small galaxy groups. For example, our results suggest that dynamical models of the evolution of galaxies in small groups of galaxies with a large amount of intragroup matter (e.g. Athanassoula et al. 1997) or with a cuspy profile for a common halo (e.g. Villalobos et al. 2012) are not fully consistent with our findings. The physical compact halo associations found here are not in virial equilibrium, but in a collapsing state, so conclusions reached about the dynamical time scale for the merging of groups, based on a

common homogeneous and virialized halo (Athanassoula et al. 1997), may not be robust. Similarly, the effects of the group environment modeled as a cuspy dark halo on the evolution of the discs (Villalobos et al. 2012) may be subject to. uncertainties. On the other hand, dynamical models of small groups where no common dark halo exists and which are in a collapsing state (e.g. Barnes 1985, Aceves & Velázquez 2002) would appear to be more consistent with the picture obtained here from the cosmological simulations. Researchers of the dynamics of groups and galaxies in such environments (IAs and LAs) may consider that about 40% of the total mass of the system is in a common rather homogeneous dark halo, (and about 20% when modeling compact associations).

As indicated in § 2.2.2 the properties of small galaxy-like groups are dependent on the algorithm chosen to determine them. Several works in the literature have constructed group catalogues in recent years (e.g. Berlind et al. 2006, Yang et al. 2007, Domínguez-Romero et al. 2012). In broad terms, for example (Berlind et al. 2005) determine groups of halos (or galaxies) in the SDSS redshift survey by looking initially for systems of galaxies that occupy a *common* dark halo; defined as a gravitationally bound structure with a typical cosmological overdensity of 200, which may include a galaxy, a group, or a cluster of galaxies. The groups they find inside such overdensities are further tested for being in virial equilibrium after obtaining small crossing times (small in comparison to the Hubble time).

Our groups of galaxy-size dark halos are not in virial equilibrium, although they have very small dimensionless crossing times. We believe the difference from the results of, for example, (Berlind et al. 2006) stems from the adopted definitions of what constitutes a group. We do not use a common halo approach but agglomerations of galaxy-size dark halos to define a group. Unfortunately, we are not aware of any work on groups that study the distribution of IG dark matter, so this precludes any appropriate comparison. Nonetheless, we made the following numerical exploration to have an idea of what to expect. We identified all virialized halos, defined as having an overdensity contrast of 200, with total mass $M \in [4M_{\rm min}, 6M_{\rm max}] \sim 10^{13}h^{-1}M_{\odot}$; similar to that of a typical group of galaxies. We found that all these systems had a central halo with some subhalos; as the one shown in Figure 10. As one would expect, in this way of determining a group, there is a deficit of IG dark matter at the center since all dark particles belong to the main halo.

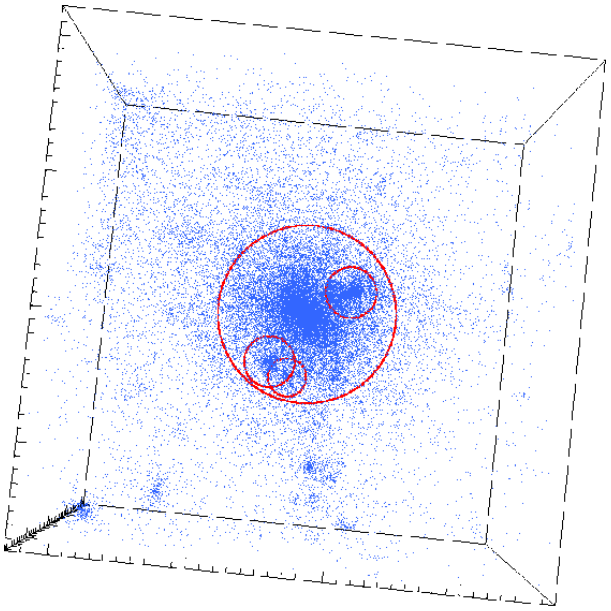

Fig. 10. Dark halo of mass $M \sim 10^{13}h^{-1}M_{\odot}$ with subhalos at $z = 0$. The outer bigger red circle depicts the virial radius of the halo, and the other red circles are the virial radius of the subhalos. Box size is $2\,h^{-1}$Mpc on each side. In this case, there is no intragroup dark matter since all dark particles belong to the main halo. The color figure can be viewed online.

We followed here what we considered a more direct approach, probably more closely resembling standard observational methods, namely: identify halos that can host normal galaxies, look for agglomerates of them within a suitable spatial scale, irrespective of whether they are part or not of a bigger common dark halo, and check whether they are physically bound or not. Our physical groups of halos, although having small dimensionless crossing times, were all in a collapsing state.

In the future, we plan to explore in more detail the intragroup dark matter properties of galaxy associations obtained by different methods, such as those indicated above; however, this is beyond the scope of the present work. The dynamical fate of our groups of halos is being explored at the present.

This research was funded by UNAM-PAPIIT and CONACyT Research Projects IN108914 and 179662, respectively. We warmly thank Martín Crocce for communications regarding cosmological initial conditions, Alexander Knebe for his help with the the AHF halo finder, and an anonymous Referee for useful comments to improve this work. We also

thank Elena Jiménez-Bailón for comments and Irving Álvarez-Castillo, from DGCTIC-UNAM, for his help with software matters.

REFERENCES

Aceves, H., & Velázquez, H. 2002, RMxAA, 38, 199
Aguerri, J. A. L., Castro-Rodríguez, N., Napolitano, N., Arnaboldi, M., & Gerhard, O. 2006, A&Ap, 457, 771
Allam, S. S., & Tucker, D. L. 2000, Astronomische Nachrichten, 321, 101
Athanassoula, E., Makino, J., & Bosma, A. 1997, MNRAS, 286, 825
Barnes, J. 1985, MNRAS, 215, 517
Barnes, J. E. 1989, Nature, 338, 123
Bartelmann, M. 2010, Classical and Quantum Gravity, 27, 233001
Berlind, A. A., Frieman, J., Weinberg, D. H., et al. 2006, ApJS, 167, 1
Brough, S., Forbes, D. A., Kilborn, V. A., & Couch, W. 2006, MNRAS, 370, 1223
Calvi, R., Poggianti, B. M., & Vulcani, B. 2011, MNRAS, 416, 727
Carlberg, R. G., Yee, H. K. C., Morris, S. L., et al. 2001, ApJ, 552, 427
Carollo, C. M., Cibinel, A., Lilly, S. J., et al. 2013, ApJ, 776, 71
Casagrande, L., & Diaferio, A. 2006, MNRAS, 373, 179
Chernin, A. D., & Mikkola, S. 1991, MNRAS, 253, 153
Crocce, M., Pueblas, S., & Scoccimarro, R. 2006, MNRAS, 373, 369
Da Rocha, C., & Mendes de Oliveira, C. 2005, MNRAS, 364, 1069
de Carvalho, R. R., Gonçalves, T. S., Iovino, A., et al. 2005, AJ, 130, 425
Deng, X.-F., He, J.-Z., Ma, X.-S., Jiang, P., & Tang, X.-X. 2008, Central European Journal of Physics, 6, 185
Diaferio, A., Geller, M. J., & Ramella, M. 1994, AJ, 107, 868
Díaz-Giménez, E., & Mamon, G. A. 2010, MNRAS, 409, 1227
Díaz-Giménez, E., Mamon, G. A., Pacheco, M., Mendes de Oliveira, C., & Alonso, M. V. 2012, MNRAS, 426, 296
Domínguez Romero, M. J. d. L., García Lambas, D., & Muriel, H. 2012, MNRAS, 427, L6
Duarte, M., & Mamon, G. 2014, arXiv:1401.0662
Efron B., Tibshirani R.J., 1993, An Introduction to the Bootstrap. Chapman & Hall, New York.
Eke, V. R., Baugh, C. M., Cole, S., et al. 2004, MNRAS, 348, 866
Elahi, P. J., Thacker, R. J., & Widrow, L. M. 2011, MNRAS, 1480
Gill, S. P. D., Knebe, A., & Gibson, B. K. 2004, MNRAS, 351, 399
Godłowski, W., & Flin, P. 2010, ApJ, 708, 920
Gómez-Flechoso, M. A., & Domínguez-Tenreiro, R. 2001, ApJ, 549, L187
Gonzalez, A. H., Zabludoff, A. I., Zaritsky, D., & Dalcanton, J. J. 2000, ApJ, 536, 561
Governato, F., Tozzi, P., & Cavaliere, A. 1996, ApJ, 458, 18
Gunn, J. E., & Gott, J. R., III 1972, ApJ, 176, 1
Han, J., Jing, Y. P., Wang, H., & Wang, W. 2012, MNRAS, 427, 2437
Hernquist, L., Katz, N., & Weinberg, D. H. 1995, ApJ, 442, 57
Hickson, P. 1997, ARAA, 35, 357
Hoekstra, H., Franx, M., Kuijken, K., et al. 2001, ApJ, 548, L5
Holmberg, E. 1950, Meddelanden fran Lunds Astronomiska Observatorium Serie II, 128, 1
Huchra, J. P., & Geller, M. J. 1982, ApJ, 257, 423
Knebe, A., Wagner, C., Knollmann, S., Diekershoff, T., & Krause, F. 2009, ApJ, 698, 266
Knebe, A., Knollmann, S. R., Muldrew, S. I., et al. 2011, MNRAS, 415, 2293
Knollmann, S. R., & Knebe, A. 2009, ApJS, 182, 608
Larson, D., Dunkley, J., Hinshaw, G., et al. 2011, ApJS, 192, 16
Lee, B. C., Allam, S. S., Tucker, D. L., et al. 2004, AJ, 127, 1811
Lewis, A., Challinor, A., & Lasenby, A. 2000, ApJ, 538, 473
Limousin, M., Cabanac, R., Gavazzi, R., et al. 2009, A&Ap, 502, 445
Mamon, G. A. 2008, A&Ap, 486, 113
McConnachie, A. W., Ellison, S. L., & Patton, D. R. 2008, MNRAS, 387, 1281
McKean, J. P., Auger, M. W., Koopmans, L. V. E., et al. 2010, MNRAS, 404, 749
Mendel, J. T., Ellison, S. L., Simard, L., Patton, D. R., & McConnachie, A. W. 2011, MNRAS, 418, 1409
Mo, H., van den Bosch, F. C., & White, S. 2010, Galaxy Formation and Evolution. Cambridge University Press, 2010.
Newman, A. B., Treu, T., Ellis, R. S., & Sand, D. J. 2013, ApJ, 765, 25
Niemi, S.-M., Nurmi, P., Heinämäki, P., & Valtonen, M. 2007, MNRAS, 382, 1864
Nolthenius, R., & White, S. D. M. 1987, MNRAS, 225, 505
Parker, L. C., Hudson, M. J., Carlberg, R. G., & Hoekstra, H. 2005, ApJ, 634, 806
Paz, D. J., Sgró, M. A., Merchán, M., & Padilla, N. 2011, MNRAS, 414, 2029
Sand, D. J. and Treu, T. and Smith, G. P. and Ellis, R. S. 2004, ApJ, 604,88
Sommer-Larsen, J. 2006, MNRAS, 369, 958
Springel, V. 2005, MNRAS, 364, 1105
Springel, V., White, S. D. M., Jenkins, A., Frenk, C. S. et al. 2005, Nature, 435, 629
Tago, E., Saar, E., Tempel, E., et al. 2010, A&Ap, 514, A102
Tatekawa, T., & Mizuno, S. 2007, JCAP, 12, 14

Tempel, E., Tamm, A., Gramann, M., et al. 2014, arXiv:1402.1350
Thanjavur, K., Crampton, D., & Willis, J. 2010, ApJ, 714, 1355
Tovmassian, H. M., Martinez, O., & Tiersch, H. 1999, A&Ap, 348, 693
Tovmassian, H., Plionis, M., & Torres-Papaqui, J. P. 2006, A&Ap, 456, 839
Tully, R. B. 1980, ApJ, 237, 390
Tully, R. B. 1987, ApJ, 321, 280
Vale, A., & Ostriker, J. P. 2004, MNRAS, 353, 189
Villalobos, Á., De Lucia, G., Borgani, S., & Murante, G. 2012, MNRAS, 424, 2401
Williams, R. J., Kelson, D. D., Mulchaey, J. S., et al. 2012, ApJ, 749, L12
Yang, X., Mo, H. J., van den Bosch, F. C., et al. 2007, ApJ, 671, 153
Zwicky, F. 1951, PASP, 63, 61

H. Aceves, L. Altamirano-Dévora, R. Cañas, F. G. Ramón-Fox and M. Reyes-Ruiz: Instituto de Astronomía, Universidad Nacional Autónoma de México, Apdo. Postal 106, C.P. 22800 Ensenada, B. C., México (aceves@astro.unam.mx).